Corrosion Behavior of Steel-Reinforced Green Concrete Containing Recycled Coarse Aggregate Additions in Sulfate Media

Abigail Landa-Sánchez [1], Juan Bosch [2], Miguel Angel Baltazar-Zamora [3,*], René Croche [4], Laura Landa-Ruiz [3], Griselda Santiago-Hurtado [5], Victor M. Moreno-Landeros [5], Javier Olguín-Coca [6], Luis López-Léon [6], José M. Bastidas [7], José M. Mendoza-Rangel [8,*], Jacob Ress [2] and David. M. Bastidas [2,*]

1. Facultad de Ingeniería Mecánica y Eléctrica, Doctorado en Ingeniería, Universidad Veracruzana, Xalapa 91000, Veracruz, Mexico; liagiba07@hotmail.com
2. National Center for Education and Research on Corrosion and Materials Performance, NCERCAMP-UA, Department of Chemical, Biomolecular, and Corrosion Engineering, The University of Akron, 302 E Buchtel Ave, Akron, OH 44325, USA; jb394@zips.uakron.edu (J.B.); jtr45@zips.uakron.edu (J.R.)
3. Facultad de Ingeniería Civil—Xalapa, Universidad Veracruzana, Lomas del Estadio S/N, Zona Universitaria, Xalapa 91000, Veracruz, Mexico; lalanda@uv.mx
4. Facultad de Ingeniería Mecánica y Eléctrica, Universidad Veracruzana, Xalapa 91000, Veracruz, Mexico; rcroche@uv.mx
5. Facultad de Ingeniería Civil—Unidad Torreón, UADEC, Torreón 27276, Mexico; grey.shg@gmail.com (G.S.-H.); vmmorlan@gmail.com (V.M.M.-L.)
6. Grupo de Investigación DICSO, Instituto de Ciencias Básicas e Ingeniería, UAEH, Hidalgo 42082, Mexico; jolguin77@gmail.com (J.O.-C.); luis_lopez@uaeh.edu.mx (L.L.-L.)
7. National Centre for Metallurgical Research (CENIM), CSIC, Ave. Gregorio del Amo 8, 28040 Madrid, Spain; bastidas@cenim.csic.es
8. Facultad de Ingeniería Civil, Universidad Autónoma de Nuevo León, Ave. Pedro de Alba S/N, Ciudad Universitaria, San Nicolás de los Garza 66455, Mexico
* Correspondence: mbaltazar@uv.mx (M.A.B.-Z.); jmmr.rangel@gmail.com (J.M.M.-R.); dbastidas@uakron.edu (D.M.B.); Tel.: +52-2282-5252-94 (M.A.B.-Z.); +1-330-972-2968 (D.M.B.)

Abstract: Novel green concrete (GC) admixtures containing 50% and 100% recycled coarse aggregate (RCA) were manufactured according to the ACI 211.1 standard. The GC samples were reinforced with AISI 1080 carbon steel and AISI 304 stainless steel. Concrete samples were exposed to 3.5 wt.% Na_2SO_4 and control (DI-water) solutions. Electrochemical testing was assessed by corrosion potential (E_{corr}) according to the ASTM C-876-15 standard and a linear polarization resistance (LPR) technique following ASTM G59-14. The compressive strength of the fully substituted GC decreased 51.5% compared to the control sample. Improved corrosion behavior was found for the specimens reinforced with AISI 304 SS; the corrosion current density (i_{corr}) values of the fully substituted GC were found to be 0.01894 $\mu A/cm^2$ after Day 364, a value associated with negligible corrosion. The 50% RCA specimen shows good corrosion behavior as well as a reduction in environmental impact. Although having lower mechanical properties, a less dense concrete matrix and high permeability, RCA green concrete presents an improved corrosion behavior thus being a promising approach to the higher pollutant conventional aggregates.

Keywords: corrosion; AISI 304 SS; AISI 1018 CS; green concrete; recycled coarse aggregate; sugar cane bagasse ash; Na_2SO_4

1. Introduction

Traditionally, the world's most widely used building material is hydraulic concrete that, when combined with AISI 1018 carbon steel (CS) rebars, forms a system known as reinforced concrete. Reinforced concrete structures are known for their long-lasting service life and low-maintenance requirements. However, due to the corrosion of the steel reinforcement, billions of dollars are spent in the repair and maintenance of bridges, tunnels, roads and docks, among others, by each country [1–5]. The corrosion of steel embedded in concrete is an electrochemical process in which the oxidation of iron occurs at the anode, whereas at the cathode, oxygen reduction takes place. Corrosion occurs due to several factors that promote passivity breakdown, primarily the carbonation or the ingress of aggressive ions [6,7]. The aggressive depassivating ions are chlorides, present in marine environments [8–10] and sulfates from inorganic salts normally present in both groundwater and in surface water. However, the concentration of aggressive agents in these environments can be highly variable [11–14]. The presence of sulfates in contact with a hardened cement paste can significantly increase the solubility of matrix components and cause degradation of concrete through leaching, thus decreasing the degree of protection of the reinforcement [15–17]. In other studies, laboratory simulations also show that the galvanized reinforcements outperform traditional carbon steel reinforcements not only in aggressive environments, but also in contact with contaminants found in the concrete mixture [18–21].

Presently, the use of ordinary Portland cement (OPC) is responsible for 10% of global CO_2 emissions, a value that can increase up to 15% in the near future [22]. As a solution to this highly pollutive binder, different approaches combining reduced greenhouse emissions and acceptable corrosion resistance properties have been proposed, such as new alkali-activated materials. Some examples of these novel binders are fly ash (FA), slags, metakaolin sugar cane bagasse ash (SCBA) or rice husks ashes (RHA), among others [19,20]. Interest in SCBA and RHA has recently increased due to the fact that both are an agricultural waste product with a similar corrosion performance to OPC [23,24]. After being treated, the SCBA shows pozzolanic activity, making it a suitable binder to replace OPC [24]. However, the required post-treatment to obtain the binder can increase the greenhouse emissions or decrease the workability of the concrete, apart from the mechanical and chemical properties as presented by Franco-Luján et al. [25]. Regarding corrosion behavior, few studies can be found considering these novel binders. For instance, FA in some studies presents a lower diffusion coefficient than OPC [26,27]. Although SCBA presents lower workability, substitution of OPC ranging between 10% and 30% reduces not only the diffusion coefficient of chloride ions, but also the permeability [25,28–32]. As a result, their use has been limited to supplementary cementitious materials (SCMs) as a conservative solution due to the lack of agreement on their corrosion performance [26–38]. This partial replacement of the OPC presents an environmentally friendly and cost-effective approach due to the by-product's nature of the novel binders [39–42].

Furthermore, the recycling of concrete is considered a key process in the current sustainable development trends. This is because concrete is widely used as a construction material. Its manufacturing consumes a large amount of nonrenewable natural resources: aggregates (80%), OPC (10%), SCM (3%) and water (7%). The natural aggregates (NA) used in the manufacturing of concrete are inert granular materials such as sand, gravel, or crushed stone. Gravel and natural sand are generally obtained from a well, river, lake, or seabed [43]. Currently, the global production of aggregates is estimated to be 40 trillion tons, which leads to the exhaustion of natural resources, high energy consumption and extreme impacts on the environment [44].

For the aforementioned reasons, recycled coarse aggregate (RCA) as a replacement for natural coarse aggregate (NCA), in addition to replacing OPC by 20% with SCBA, represents a substantial reduction in the environmental impact of concrete manufacturing [44]. This topic is of great concern in Europe and in developed countries such as the USA and Canada, among others [45]. A total of 78,000 tons of RCA were used in the Netherlands in 1994, due to the fact that the use of 20% RCA thick did not differentiate properties of fresh or hardened concrete, according to the corresponding

national organization [46]. The increasing trend of research efforts of RCA for the manufacturing of new concrete has also increased the interest in the production of high-performance, high-strength concrete [47]. It should be noted that the use of thick RCA (up to 30%) is usually recommended, but it is often considered necessary to add superplasticizers [48] to achieve the required workability of the new concrete. These materials can improve the durability of concrete [44–54]. Due to the scarce works found in the literature, further research efforts are needed to determine the effect of the RCA as well as the partial substitution of OPC with SCBA in the corrosion performance of these novel concretes [55–57].

The aim of this work was to study the effect of the substitution of NCA by the environmentally friendly RCA on the GC embedding AISI 1018 carbon steel (CS) and AISI 304 SS rebars. This GC was also partially substituted with SCBA to further decrease the environmental impact of the traditional OPC concrete. Furthermore, the mechanical strength of the new GC was investigated to describe its future real-world applications. Five different concrete mixtures were prepared according to the ACI 211.1 standard [58], two reinforcement alloys, AISI 304 SS and carbon steel 1018, were investigated under control and aggressive environments. Corrosion monitoring techniques, such as open circuit potential (OCP) and linear polarization resistance (LPR), were used to elucidate the corrosion behavior of the novel green concretes. This work contributes to the corrosion performance knowledge as there is not a clear mechanism on how RCA affects the corrosion phenomenon. Furthermore, it presents concrete mixtures with a substantial reduction in the environmental impact due to the partial substitution not only of OPC with SCBA, but also the natural aggregates by the RCA, thus reducing the CO_2 emissions substantially [22].

2. Materials and Methods

2.1. Green Concrete (GC)

Three different concrete mixtures were made: a conventional concrete control mixture (MC) made with 100% OPC following the standard for Portland blended cement (CPC 30R, NMX-C-414-ONNCCE-2014) [59], natural fine (NFA) and coarse (NCA) aggregates and two mixtures of green concrete (GC)—the first green concrete with a 50% substitution of NCA for RCA and with a partial 20% substitution of cement for SCBA, and the second green concrete with a 100% substitution of RCA and the same SCBA ratio. The SCBA was obtained from Mahuixtlan sugar mills, located in Coatepec, Mexico. The characterization of the physical properties of aggregates, NCA, NFA and RCA, was made in accordance with the ASTM standards, the tests were relative density (specific gravity) [60,61], bulk density (unit weight, kg/m^3) [62], absorption (%) of coarse aggregate and fine aggregate [63], maximum aggregate size and fineness modulus [58]. Figure 1 shows the proposed experimental testing procedure to determine the optimal mixture design. Table 1 shows the physical properties of the materials in this research.
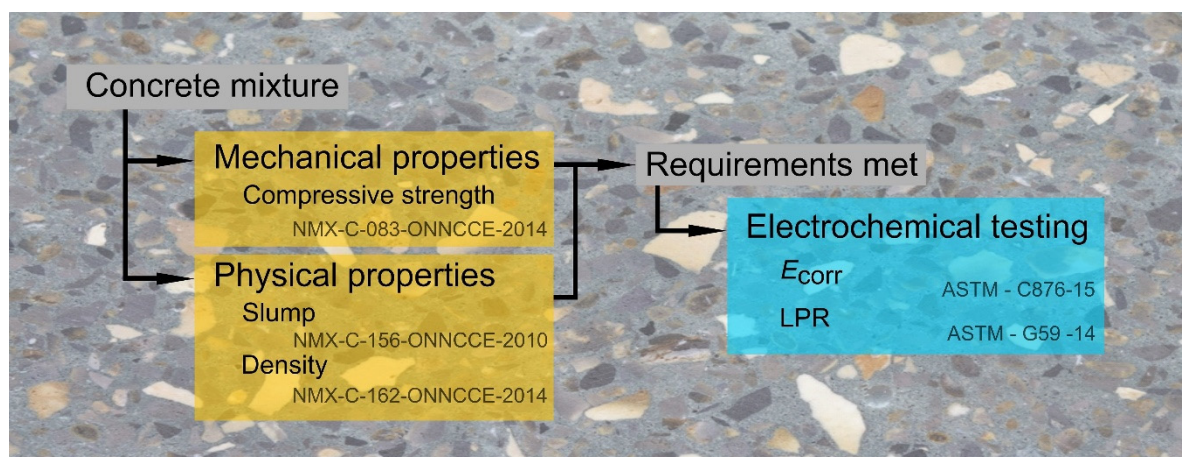

Figure 1. Experimental testing procedure schematic.

Table 1. Physical properties of the natural coarse aggregate (NCA), natural fine aggregate (NFA) and recycled coarse aggregate (RCA).

Type of Aggregates	Relative Density (Specific Gravity)	Bulk Density (Unit Weight, kg/m^3)	Absorption (%)	Fineness Modulus	Maximum Aggregate Size (mm)
NCA	2.62	1433	1.73	-	19
NFA	2.24	1695	1.85	2.2	-
RCA	2.20	1367	12.00	-	19

2.2. Design Mixtures of Conventional Concrete (MC) and GC

The design of concrete mixtures for MC and GC created according to the standard ACI 211.1 [58]. This standard describes a method that is based on the physical properties of coarse and fine aggregates (see Table 1). The proportioning of the concrete mixture indicates the amount of material needed to produce a meter cubic of concrete. In this case, the manufacture of the three concrete mixes used a water/cement ratio of 0.65 for a specified compressive strength of concrete (f'_c = 22.5 MPa according to ACI 214R-11 [64]). Table 2 summarizes the proportions for the MC and the two GC mixtures (M50 and M100).

Table 2. Proportioning of concrete mixtures in kg for 1 m^3 of concrete (f'_c = 22.5 MPa).

Materials	MC (100% CPC)	M50 (50% RCA)	M100 (100% RCA)
	Kg/m^3		
Cement	315	252	252
Water	205	205	205
SCBA	0	63	63
NCA	917	458.5	0
NFA	914	914	914
RCA	0	458.5	917

2.3. Physical and Mechanical Properties of Concrete Mixtures (Fresh and Hardened State)

For the evaluation of the physical properties of fresh-state concrete mixtures, tests of slump [65], freshly mixed concrete temperature [66] and density [67] were carried out according to the ONNCCE and ASTM standards. Table 3 shows the results obtained for the two concrete mixtures.

Table 3. Physical properties of concrete mixtures.

Concrete Mixture	Slump (cm)	Temperature (°C)	Density (kg/m^3)
MC	10 cm	24	2220
M50	3 cm	19	2187
M100	2 cm	22	2040

To determine the mechanical strength (compressive strength, f'_c) of the concrete mixtures in the hardened state, compression tests were carried out according to the standard NMX-C-083-ONNCCE-2014 [68], at the ages of 14 and 28 days. Table 4 shows the results obtained.

Table 4. Compressive strength at 14 and 28 days (f'_c in MPa).

Concrete Mixture	Compressive Strength (MPa)	
	14 Days	28 Days
MC	14.02	19.91
M50	7.71	11.54
M100	6.75	9.66

The compressive strength decreased as the content of recycled coarse aggregate (RCA) present in GC increased. The GC mix with 50% RCA and 20% SCBA was substituted for the cement CPC 30R (M50) and showed a compressive strength of 11.54 MPa at 28 days. This represents a decrease of 42% with respect to the MC, and a decrease of 51.5% for GC with 100% RCA and 20% SCBA replacing cement CPC 30R, reporting a compressive strength of only 9.66 MPa at an age of 28 days. The decrease in compressive strength in GC mixes is related to the incorporation of RCA. This behavior agrees with that reported in various investigations. Ali et al. found in their investigation of glass fibers incorporated in concrete with RCA that when RCA completely replaces NCA, it reduces the compressive strength, split tensile strength and flexure strength by about 12%, 11% and 8%, respectively [69]. Kurda et al. concluded that both materials, FA and RCA, are detrimental to the mechanical properties of concrete. For instance, compressive strength, splitting tensile strength and modulus of elasticity are negatively affected. The SiO_2 present in the FA and the $Ca(OH)_2$ present in the RCA experience a pozzolanic reaction that increases the rate of concrete strength development over time [70]. The SiO_2 is also present in the SCBA according to previous results [71], thus being a likely source of this detrimental behavior. Li et al. explained in their research in the structural area that there is a reasonable consensus regarding the structural behavior of composite members combined with RCA. Mechanical strength is slightly lower compared with OPC with no RCA additions. Nevertheless, the manufacturing of composite materials using RCA presents a safe and feasible approach [72]. However, the compressive strength observed for GC was sufficient for use in structures that do not require high strength, such as houses, parks, sidewalks, floors, etc.

2.4. Specifications, Characteristic and Nomenclature of Specimens for Electrochemical Tests

The MC and the two mixtures of GC (M50 and M100) were made with a water/cement ratio of 0.65. The specimens were prisms with dimensions of $15 \times 15 \times 15$ cm. In all the specimens, AISI 304 SS and AISI 1018 CS rebars were embedded with a length of 15 cm and a diameter of 9.5 mm; the AISI 304 SS and AISI 1018 CS rebars were cleaned to remove any impurities [73]. In addition, each rebar was coated 4 cm from the top and 4 cm from the bottom using insulating tape in order to limit the exposed area with a length of 5 cm, as reported previously [74,75].

The specimens were manufactured in accordance with the standard ASTM C 192 [76] and the curing stage of all specimens was carried out water immersion according to the NMX-C-159 standard [77]. After the curing period, the eight specimens were placed in the exposure media, a control medium (DI-water) and 3.5 wt.% Na_2SO_4 solution for 364 days, simulating a sulfate aggressive medium such as contaminated soils, marine and industrial environments [78,79]. The specimens were then subjected to electrochemical tests. Figure 2 shows the compressive strength tests of the different GC mixtures and the electrochemical test to determine the corrosion behavior after exposure to 3.5 wt.% Na_2SO_4 solution.

Table 5 shows the elemental composition of the austenitic AISI 304 stainless steel and AISI 1018 carbon steel.

The nomenclature used for the electrochemical monitoring of AISI 304 SS and AISI 1018 CS embedded in the MC and the two GC (M50 and M100) exposed in a control medium (DI-water) and 3.5 wt.% Na_2SO_4 solution is shown in Table 6, which has the following meaning:

- MC, M50 and M100 indicate the concrete mixture (conventional and green concrete);
- W indicates exposed DI-water (control medium);
- S indicate exposed to 3.5 wt.% Na_2SO_4 solution (aggressive medium);
- 18 for rebars of AISI 1018 CS;
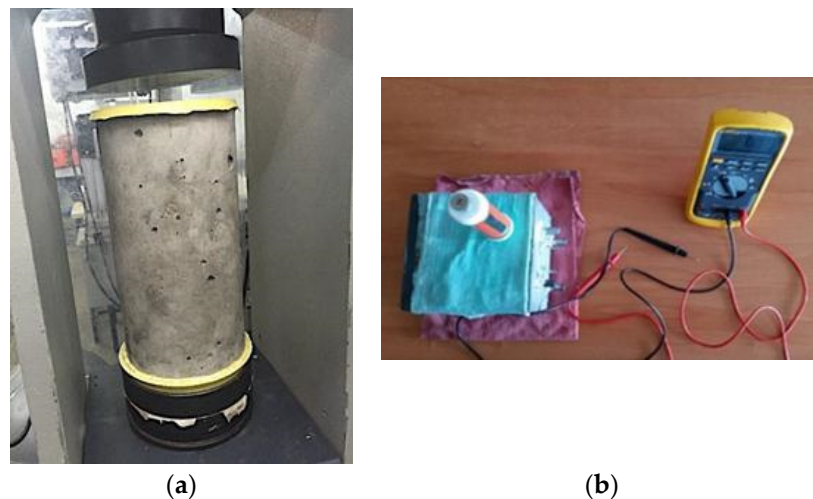- 304 for rebars of AISI 304 SS.

Figure 2. Experimental test conducted on green concrete: (**a**) compressive strength and (**b**) electrochemical corrosion monitoring.

Table 5. Elemental composition (wt.%) of the reinforcements tested, AISI 1018 carbon steel (CS) and austenitic AISI 304 SS.

Material	Element, wt.%									
	C	Si	Mn	P	S	Cr	Ni	Mo	Cu	Fe
AISI 1018	0.20	0.22	0.72	0.02	0.02	0.13	0.06	0.02	0.18	Balance
AISI 304	0.04	0.32	1.75	0.03	0.001	18.20	8.13	0.22	0.21	Balance

Table 6. Nomenclature of the reinforced green concrete specimens for electrochemical monitoring.

Mixtures Concrete	Nomenclature of Specimens Exposed DI-Water (Control Medium)		Nomenclature Specimens Exposed to 3.5 wt.% Na$_2$SO$_4$ Solution (Aggressive Medium)	
MC (Conventional Concrete: 100% NA and 100% CPC)	MC-W-18	MC-W-304	MC-S-18	MC-S-304
M50 (Green Concrete: 50% RCA and 20% SBCA)	M50-W-18	M50-W-304	M50-S-18	M50-S-304
M100 (Green Concrete: 100% RCA and 20% SBCA)	M100-W-18	M100-W-304	M100-S-18	M100-S-304

MC and GC specimens were exposed to two different media, the control medium (DI-water) and 3.5 wt.% Na$_2$SO$_4$ solution, for a period of 364 days. The corrosion behavior was characterized by corrosion potential (E_{corr}) and corrosion current density (i_{corr}) measurements. The electrochemical cell setup used was AISI 304 SS or AISI 1018 CS rebars with a diameter of 9.5 mm for working electrodes (WE). AISI 314 SS rebars were used as counter electrodes (CE; see Figure 3) and standard copper–copper sulfate (Cu/CuSO$_4$, CSE) as the reference electrode (RE). i_{corr} was monitored using the linear polarization resistance (LPR) technique. The sweep potential range was ±20 mV with respect to the E_{corr} and the sweep rate was 10 mV/min according to standard ASTM-G59 [80]. Electrochemical measurements were performed in a Gill AC Galvanostat/Potentiostat/ZRA (ACM Instruments, Cark in Cartmel, UK). The results were analyzed using Version 4 Analysis specialized

software from ACM Instruments [81,82]. All tests were carried out at room temperature. E_{corr} and i_{corr} were monitored every four weeks and all experimental measurements were performed in triplicate.
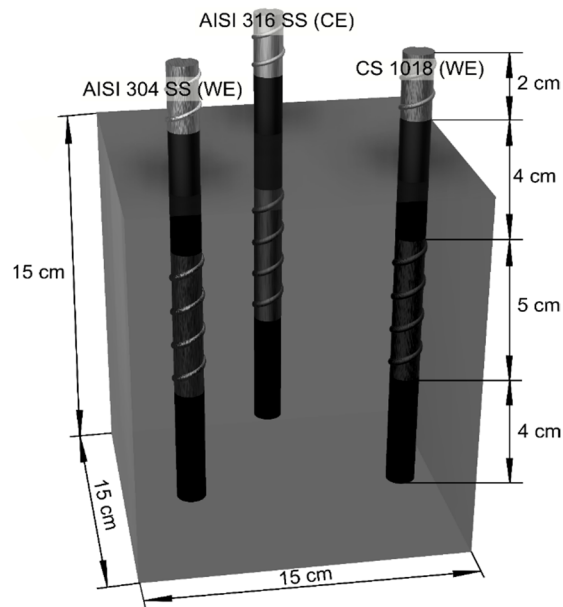

Figure 3. Specifications of specimens for electrochemical tests.

The i_{corr} and the corrosion rate (v_{corr}) were estimated from the LPR technique using the Stern and Geary relation (see Equation (1)) [83]:

$$i_{corr} = \frac{B}{R_p} \tag{1}$$

where B is the proportionality constant equal to 26 and 52 mV/dec for active and passive corrosion state rebars, respectively, and R_p is the polarization resistance [84,85].

E_{corr} was used to assess the degree of deterioration of reinforced concrete specimens according to ASTM C-876-15 [86], which presents the criteria or ranges that relate the E_{corr} values with the probability of corrosion for embedded steel specimens made with MC and GC (see Table 7).

Table 7. The measured half-cell corrosion potential (E_{corr}) versus a Cu/CuSO$_4$ in reinforcement concrete [86].

E_{corr} (mV$_{CSE}$)	Corrosion Condition
$E_{corr} > -200$	Low (10% of risk corrosion)
$-200 > E_{corr} > -350$	Intermediate corrosion risk
$-350 > E_{corr} > -500$	High (<90% of risk corrosion)
$E_{corr} < -500$	Severe corrosion

To determine the v_{corr} values of steels embedded in the mixtures of MC and GC, the i_{corr} values were used. The criteria used to analyze the i_{corr} results are based on the state of corrosion of CS in OPC reported in the literature [84], as shown in Table 8.

Table 8. Level of corrosion in concrete, corrosion current density (i_{corr}) and the corrosion rate (v_{corr}) [84].

i_{corr} (μA/cm^2)	v_{corr} (mm/d)	Corrosion Level
$i_{corr} \leq 0.1$	$v_{corr} \leq 0.001$	Negligible (Passivity)
$0.1 < i_{corr} < 0.5$	$0.001 < v_{corr} < 0.005$	Low Corrosion
$0.5 < i_{corr} < 1$	$0.005 < v_{corr} < 0.010$	Moderate Corrosion
$i_{corr} > 1$	$v_{corr} > 0.010$	High Corrosion

3. Results and Discussion

3.1. Half-Cell Potential—Corrosion Potential

Half-cell potential monitoring (E_{corr}) and interpretation of the corrosion state were performed using the criteria presented in Table 7, which is in accordance with ASTM C876-15 [86].

3.1.1. E_{corr} Specimens Exposed DI-Water (Control Medium)

Figure 4 shows the results obtained from monitoring the E_{corr}, of the specimens MC-W-18, M50-W-18 and M100-W-18. It is observed that the MC-W-18 specimen presents corrosion potentials in the curing stage ranging from −260 to −160 mV$_{CSE}$, moving from Days 7 to 28 from the intermediate corrosion risk to 10% risk, according to ASTM C-876-15. The trend towards more positive values continued throughout the evaluation period, reaching values up to −45 mV$_{CSE}$ on Day 196, and finally reaching values in the range of −60 to −75 mV$_{CSE}$, which indicates a 10% of risk corrosion. For the M50-W-18 specimen, the behavior is very similar to the MC-W-18 specimen, with E_{corr} values in the curing stage of −250 mV$_{CSE}$, reaching a value of −140 mV$_{CSE}$ on Day 28, maintaining a trend towards more positive values until Day 196, reaching an E_{corr} value of −45 mV$_{CSE}$. At the end of the monitoring period, more negative E_{corr} values are found ranging between −120 and −145 mV$_{CSE}$, thus indicating a 10% corrosion risk.

The M100-W-18 specimen shows a more unfavorable behavior from Day 196, from E_{corr} values lower than −200 = to −330 mV$_{CSE}$ for Day 280, until values of −300 mV$_{CSE}$ observed at the end of the monitoring period. Therefore, the specimens indicate intermediate corrosion risk according to ASTM C-876-15 and with a tendency to more negative values of E_{corr}, which agrees with the findings of Al-Yaqout et al.; the corrosion potential for normal mixtures decreases as the RCA replacement level increases compared to the control mixture. This behavior shows the same trend for the compressive strength, decreasing as the amount of RCA increased in all normal and slag mixtures and under all exposure conditions [87].

The MC-W-304 (MC, 100% CPC-100% natural aggregates), M50-W-304 (GC with 50% RCA and 80% CPC-20% SCAB) and M100-W-304 (GC with 100% RCA and 80% CPC-20% SCAB) specimens were reinforced with AISI 304 SS steel rebars. The E_{corr} results obtained after more than 360 days of monitoring show the following behavior. The MC-W-304 specimen presented a tendency to more noble E_{corr} values from the curing stage, presenting values from −192 mV$_{CSE}$ on Day 7 to −84 mV$_{CSE}$ on Day 28, continuing with a tendency to passive E_{corr} values in the range of −80 to −75 mV$_{CSE}$ from Day 196 [88,89], presenting values below or more positive than −200 mV$_{CSE}$, which indicates, according to the ASTM C-876-15, a 10% corrosion risk or passivity of the steel–concrete system analyzed.

The M50-W-304 specimen behaves similarly to the control MC-W-304, with corrosion potentials in the curing stage ranging from −218 mV$_{CSE}$ on Day 7 to −95 mV$_{CSE}$ on Day 28, presenting a small activation on Day 56 with an E_{corr} value of −143 mV$_{CSE}$. From this point to the present, a stage of stability in the E_{corr} values is observed from Days 84 to 364, in the range of −90 and −120 mV$_{CSE}$, interpreted according to the ASTM C-876-15 as a 10% corrosion risk. The M100-W-304 specimen, presented a similar behavior to the two MC-W-304 and M50-W-304 specimens in the curing stage, showing an E_{corr} value of −183 mV$_{CSE}$ on Day 7 and −97 mV$_{CSE}$ on Day 28. From this point on, the E_{corr} values become −82 and −124 mV$_{CSE}$ until the end of the testing, indicating according to the ASTM C-876-15 as a 10% corrosion risk. The behavior in the E_{corr} values is less than −200 and congruent with the nonaggressive medium of exposure, which is also interpreted as the passivity of the AISI 304 SS steel used as reinforcement in GC and MC.
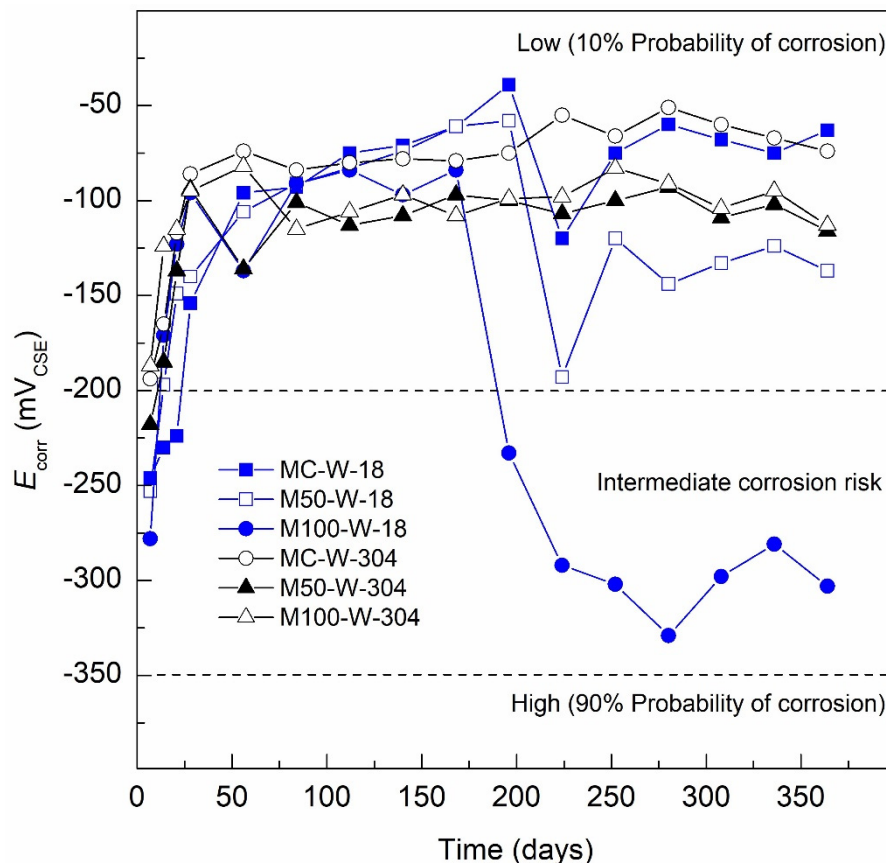
Figure 4. E_{corr} specimens exposed DI-water (control medium).

3.1.2. E_{corr} Specimens Exposed 3.5 wt.% Na_2SO_4 Solution (Aggressive Medium)

Figure 5 presents the results obtained from the E_{corr} monitoring of the specimens when exposed for 364 days to 3.5 wt.% Na_2SO_4 solution (aggressive medium). The evaluated specimens were MC-S-18 (MC, 100% CPC-100% natural aggregates), M50-S-18 (GC with 50% RCA and 80% CPC-20% SCAB) and M100-S-18 (GC with 100% RCA and 80% CPC-20% SCAB). The MC-S-18 specimen in the curing stage presented an E_{corr} value of −217 mV_{CSE} on Day 7 and −180 mV_{CSE} for Day 28. These E_{corr} values indicate, according to the ASTM C-876-15, a 10% corrosion risk. Later, the specimen presents E_{corr} values in the range from −173 to −159 mV_{CSE} after Day 112, from this point to the present, an activation occurs with E_{corr} values from −203 to −256 mV_{CSE} from Day 140 to 224, which would indicate intermediate corrosion risk according to ASTM C-876-15. For Days 252 and 280, E_{corr} values are lower than −200 mV_{CSE}, which would be associated with a passivity stage or a 10% corrosion risk; however, after Day 280, there is a trend towards more negative values of −200 mV_{CSE}, reaching −239 mV_{CSE} on the last day of monitoring. The M50-S-18 specimen presents more negative values of E_{corr} in the curing stage than those presented by the control MC-S-18 specimen, with an E_{corr} value of −261 mV_{CSE} on Day 7 and −218 mV_{CSE} for Day 28, showing from Days 56 to 140 E_{corr} values that ranged between −189 and −243 mV_{CSE}. Then, the specimen shows a decreasing trend towards lower values until the end of the testing, with values reaching −284 mV_{CSE}, after Day 140 and until the end of monitoring, Day 364, the E_{corr} values for the M50-S-18 specimen when exposed in 3.5 wt.% Na_2SO_4 solution (aggressive medium) indicate intermediate corrosion risk according to the ASTM C-876-15.
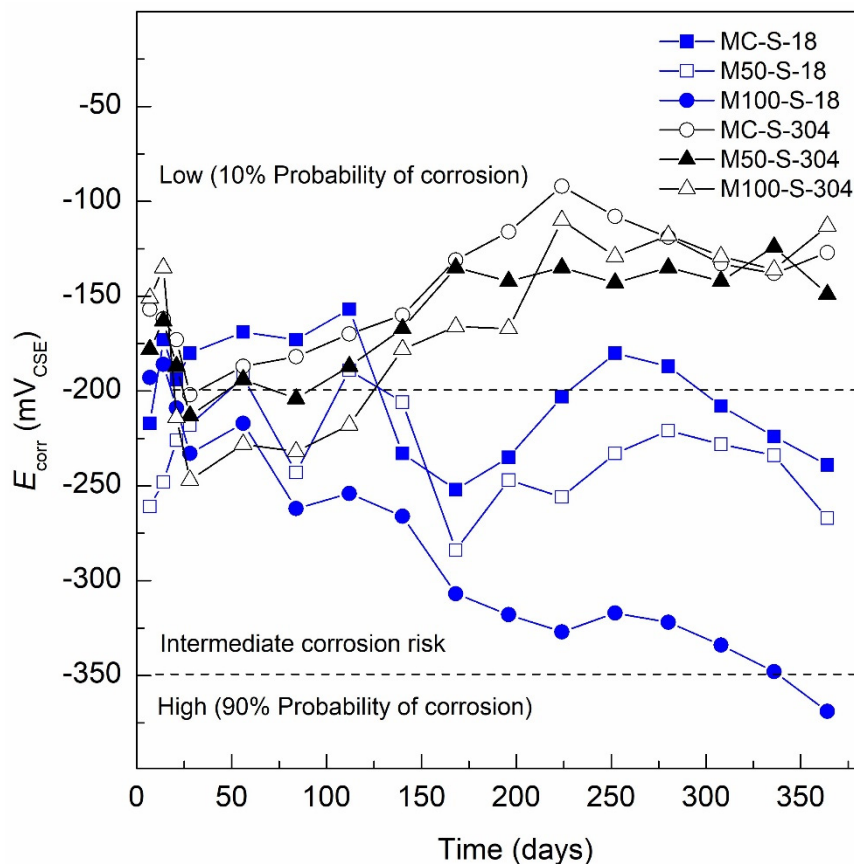
Figure 5. E_{corr} specimens exposed 3.5 wt.% Na_2SO_4 solution (aggressive medium).

The specimen that presented the worst performance when exposed to 3.5 wt.% Na_2SO_4 solution (aggressive medium) was M100-S-18, presenting a tendency to lower E_{corr} values with an E_{corr} value of −193 mV_{CSE} on Day 7 of the curing stage and −233 mV_{CSE} for Day 28, continuing with the negative trend throughout the entire exposure period, reaching a potential of −348 mV_{CSE} on Day 336 and ending on Day 364 with a corrosion potential of −369 mV_{CSE}. This indicates a <90% corrosion risk according to the ASTM C-876-15 standard. This behavior of more negative corrosion potentials (E_{corr}) coincides with that reported in other investigations when evaluating AISI 1018 steel in sustainable concrete made with SCBA and exposed to sulfates [24]. However, the M100-S-18 specimen presents more negative values, which is associated with lower corrosion resistance of the specimens made with GC (M50-S-18 and M100-S-18) when exposed to sulfates, related to a less dense matrix and higher permeability due to the presence of 50% and 100% RCA, as well as the substitution of Portland cement in 20% by SCBA. This decrease in the mechanical properties and durability when RCA has been used was reported by Lovato et al. [90], indicating that the durability properties are also negatively affected by the increment of RCA in concrete. In order to achieve the required workability, the water-to-cement ratio must be increased. This not only leads to an increased demand for water during the manufacturing stage, but also an increase in the porosity of the matrix and consequently reducing the durability of the concretes [90].

The specimens with AISI 304 SS steel were MC-S-304 (MC, 100% CPC-100% natural aggregates), M50-S-304 (GC with 50% RCA and 80% CPC-20% SCAB) and M100-S-304 (GC with 100% RCA and 80% CPC-20% SCAB), exposed for 364 days to 3.5 wt.% Na_2SO_4 solution (aggressive medium). The MC-S-304 specimen presented an E_{corr} value of −157 mV_{CSE} on Day 7 of the curing stage and −202 mV_{CSE} for Day 28, from this point, the specimen presents a trend towards higher E_{corr} values, related to the passivity of AISI 304 SS steel, and reached a minimum E_{corr} of −92 mV_{CSE} on Day 224 of exposure. Then, the specimen showed E_{corr} values in the range from −108 to −138 mV_{CSE} until

the end of the monitoring period, all the E_{corr} values of the MC-S-304 specimen during the entire period of exposure to the aggressive medium were less than −200 mV$_{CSE}$, thus indicating a 10% corrosion risk according to the ASTM C-876-15. The M50-S-304 specimen presented a behavior similar to MC-S-304, with corrosion potentials in the curing stage with a decreasing trend. The M50-S-304 specimen displays an E_{corr} value of −178 mV$_{CSE}$ on Day 7 and −213 mV$_{CSE}$ for Day 28, then increases and become more passive to −138 mV$_{CSE}$ by Day 168 and remains stable in the range of −135 and −149 mV$_{CSE}$ until the final measurement, maintaining E_{corr} values below −200 mV$_{CSE}$ throughout the exposure period, thus indicating, according to ASTM C-876-15, a 10% corrosion risk. Finally, the M100-S-304 specimen presents a similar behavior to the two previous specimens in the curing stage, with corrosion potentials ranging from less to more negative, with an E_{corr} value of −151 mV$_{CSE}$ on Day 7 and −247 mV$_{CSE}$ on Day 28. Unlike the MC-S-304 and M50-S-304 specimens, the M100-S-304 specimen presents E_{corr} values less than −200 mV$_{CSE}$ until Day 112, which would indicate intermediate corrosion risk according to the ASTM C-876-15. Thereafter, the specimen shows a trend towards higher E_{corr} values, reaching an E_{corr} value of −110 mV$_{CSE}$ for Day 224 and remaining stable in the range between −136 and −113 mV$_{CSE}$ until the end of the testing. Like the previous specimens, the M100-S-304 specimen presented E_{corr} values less than −200 mV$_{CSE}$ during almost the entire exposure time to 3.5 wt.% Na$_2$SO$_4$ solution (aggressive medium), which indicates a 10% corrosion risk according to ASTM C-876-15. The previous results agree with those reported in the literature, where the excellent corrosion resistance of stainless steel grades AISI 304, AISI 316, etc., has been demonstrated when used as reinforcement in conventional concrete, sustainable concrete, green concrete, and when exposed to aggressive environments such as marine, sulfated and industrial environments [91,92].

3.2. Corrosion Current Density, i_{corr}

The i$_{corr}$ results of the AISI 304 SS and AISI 1018 CS reinforcement in MC and both GC mixtures (M50 and M100) exposed to control medium (DI-water) and 3.5 wt.% Na$_2$SO$_4$ solution were interpreted according to the criterion of Table 8.

3.2.1. i$_{corr}$ Specimens Exposed DI-Water (Control Medium)

Figure 6 shows the i_{corr} results of the conventional concrete and GC specimens reinforced with AISI 1018 CS and AISI 304 SS steel exposed in water as a control medium. The MC-W-18 specimen presents an i_{corr} value of 0.67 µA/cm^2 for Day 7 of the curing stage, decreasing on Day 28 to a value of 0.21 µA/cm^2. For Day 56, a passive i_{corr} value of 0.095 µA/cm^2 was observed, and subsequently, values remained less than 0.091 µA/cm^2 until the end of monitoring in the range of 0.09 to 0.05 µA/cm^2. The i_{corr} values obtained from the MC-W-18 specimen indicate passivation of the reinforcing steel and, according to Table 8, a negligible level of corrosion (absence of corrosion). The M50-W-18 specimen presents a similar passivation behavior as MC-W-18; however, with higher i_{corr} values from the curing stage, presenting on Day 7 an i_{corr} value of 0.58 µA/cm^2 and 0.29 µA/cm^2 for Day 28. From Day 56 to the end of monitoring, i_{corr} values were below 0.1 µA/cm^2 in the range of 0.07 to 0.04 µA/cm^2, indicating a negligible level of corrosion. The M100-W-18 specimen had a similar behavior to the two previous specimens with an i_{corr} on Day 7 of 0.64 to 0.26 µA/cm^2 for Day 28 and presenting an i_{corr} value of 0.067 µA/cm^2 until Day 140. From Day 168 until the end of monitoring, i_{corr} values were in the range of 0.144 to 0.214 µA/cm^2, indicating a low level of corrosion according to Table 8 and supporting the corrosion potential monitoring technique. The corrosion potentials presented by the same M100-W-18 specimen, after Day 168 were in the range of −200 to −340 mV$_{CSE}$, indicating corrosion uncertainty according to ASTM C-876-15. With the LPR test, the i_{corr} could be determined, confirming the activation of the system with the presence of a low level of corrosion from Day 196 for the M100-W-18 specimen in a nonaggressive environment. The corrosion present in the M100-W-18 specimen exposed to a nonaggressive medium is related to the less dense and more permeable matrix of green concrete (M100), as indicated by the low compressive strength at 28 days with f'_c = 9.66 MPa. This decrease in the durability of concrete made with RCA has been demonstrated in

various investigations, Kurda et al. found that the water absorption increases and electrical resistivity decreases with the increasing incorporation level of RCA; the opposite occurs with the addition of FA for both tests [93]. The behavior of the i_{corr} of the other two specimens, MC-W-18 and M50-W-18, indicated a negligible level of corrosion (passivity).
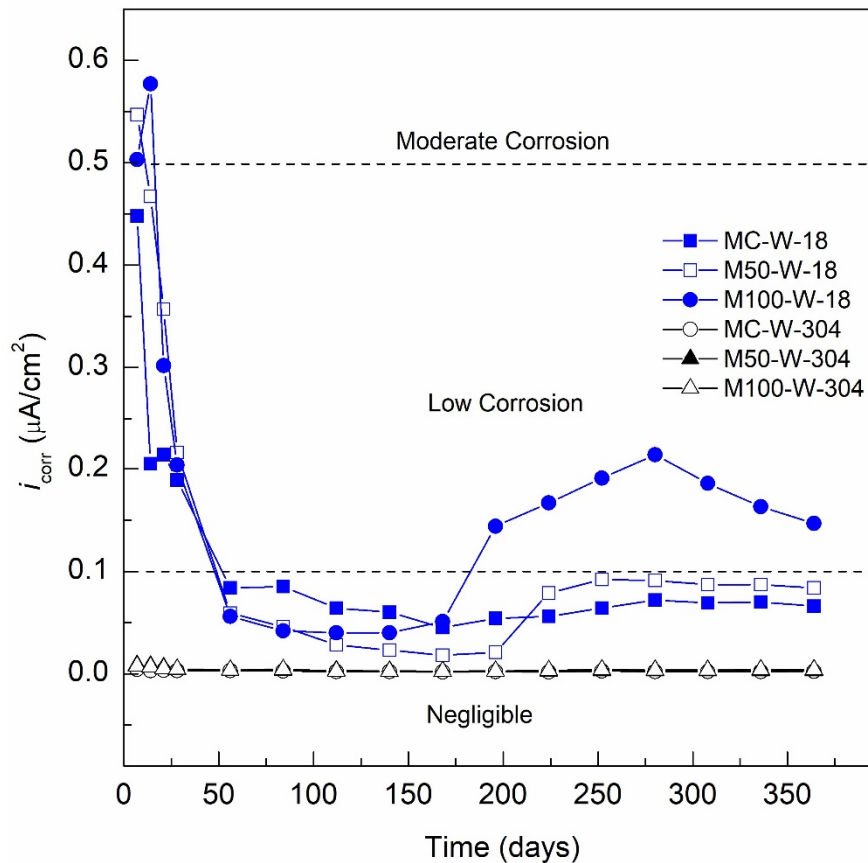

Figure 6. i_{corr} specimens exposed DI-water (control medium).

The MC-W-304 specimen in the curing stage showed an i_{corr} value of 0.0043 μA/cm^2 on Day 7 with a trend towards more passive values, presenting an i_{corr} value of 0.0031 μA/cm^2 on Day 28. A trend to lower i_{corr} values is observed until Day 224 with an i_{corr} value of 0.0018 μA/cm^2. Then, the specimen exhibits a small increase of i_{corr} to 0.0028 μA/cm^2 for Day 252 and from i_{corr} values of 0.0021 μA/cm^2 on Day 280 to 0.0023 μA/cm^2 for the last monitoring on Day 364. All i_{corr} values of the MC-W-304 specimen indicate a negligible or null corrosion level according to that indicated in Table 8. It is also found that this specimen presents the lowest i_{corr} values, followed by the M50-W-304 specimen, which presented i_{corr} values of 0.0085 μA/cm^2 on Day 7 to 0.0041 μA/cm^2 for Day 28, then continues with a decrease in i_{corr} until Day 168 with a value of 0.0023 μA/cm^2. Subsequently, the i_{corr} increases from 0.0026 to 0.0032 μA/cm^2 from Days 196 to 364, respectively. Finally, the M100-W-304 specimen (100% RCA and 20% SCBA) presented the highest i_{corr} values, presenting an i_{corr} value of 0.0045 μA/cm^2 on Day 28, decreasing to 0.0024 μA/cm^2 on Day 168. Following, i_{corr} increases from 0.0027 μA/cm^2 on Day 196 to a value of 0.0040 μA/cm^2 for the last day of monitoring, Day 364. A clear difference is observed in the i_{corr} values presented by the three studied specimens, the lowest i_{corr} values are shown for the MC-W-304 specimen, followed by the M50-W-304 specimen, and finally the M100-W-304 specimen, the i_{corr} range of the three specimens is more than 10 times less than 0.1 μA/cm^2, which indicates that all the specimens present a negligible level of corrosion throughout the period of exposure to the control medium according to Table 8. The results coincide with what is reported in the literature [21,94,95].

3.2.2. i_{corr} Specimens Exposed 3.5 wt.% Na$_2$SO$_4$ Solution (Aggressive Medium)

Figure 7 presents the v_{corr} and i_{corr} results of the specimens with AISI 304 SS and AISI 1018 CS steel bars embedded in MC and GC exposed to 3.5 wt.% Na$_2$SO$_4$ solution (aggressive medium) for a period of 364 days. The v_{corr} and i_{corr} of the control specimen, MC-S-18, decreased from an i_{corr} value of 0.2435 μA/cm^2 on Day 7 to an i_{corr} value of 0.1144 μA/cm^2 for Day 28. This behavior is attributed to being in the curing stage where the i_{corr} values tend to decrease due to the formation of the passive layer and the increase in the protection of the concrete. The i_{corr} values decrease until Day 140 of exposure with a value of 0.0729 μA/cm^2, indicating a negligible level of corrosion or passivity according to Table 8. However, after Day 168, the activation of the system occurs with a constant increase in i_{corr} values greater than 0.1 μA/cm^2 on Day 196 with an i_{corr} value of 0.1656 μA/cm^2 and reaching 0.2148 μA/cm^2 at the end of monitoring. This indicates that, as of Day 196, the MC-S-18 specimen presented corrosion at a low level due to the exposure to sodium sulfate solution as an aggressive medium. In the case of the M50-S-18 specimen, the curing stage showed decreasing i_{corr} values, reporting 0.3375 μA/cm^2 on Day 7 to 0.1844 μA/cm^2 for Day 28. This trend continued to decrease until Day 56, reaching an i_{corr} value of 0.1506 μA/cm^2. However, after Day 84, the i_{corr} values begin to increase, becoming more active due to exposure to the aggressive environment and a decreased matrix density and increased permeability because it contains 50% of RCA. The values increase to 0.2779 μA/cm^2 and remain stable in an i_{corr} range of 0.2419 and 0.3386 μA/cm^2 until the end of monitoring. From Day 84, the M50-S-18 specimen presents i_{corr} values that indicate a low level of corrosion according to Table 8. Finally, the M100-S-304 specimen, although showing a tendency for lower i_{corr} values in the curing stage, displays an i_{corr} value of 0.4175 μA/cm^2 on Day 7 and 0.2482 μA/cm^2 for Day 28. For Day 86, the activation of the system with an increase in its i_{corr} is shown, reaching a value of 0.3417 μA/cm^2. On Day 140, an i_{corr} value of 0.519 μA/cm^2 indicates a moderate level of corrosion according to Table 8. The i_{corr} increases for the M100-S-18 specimen continued irregularly from Day 168 to 308, ending on Day 364 with an i_{corr} value of 0.7389 μA/cm^2. The influence of the 100% RCA in the specimen is observed, influencing the mechanical properties and durability of GC due to a more permeable concrete matrix, lower density and a low resistance to compression compared to the control concrete (concrete with 50 and 100% of coarse natural aggregate). However, the use of mineral admixture (SF, MK, FA and ground granulated blast slag) resulted in a decrease in the charge passed through the concrete specimens [96]. According to Alhawat et al., not only the corrosion initiation process happened faster in RCA concrete, but also a higher corrosion rate was observed as the RCA content increased due to the higher porosity and water absorption [97].

The MC-S-304 specimen presents the best performance against corrosion when exposed for 364 days to 3.5 wt.% Na$_2$SO$_4$ solution (aggressive medium), reporting i_{corr} values in the curing stage of 0.0047 μA/cm^2 on Day 7 to reach an i_{corr} value of 0.0034 μA/cm^2 on Day 28, observing a decrease associated with the increase in concrete protection due to the hydration process of said stage. The decrease in the corrosion rate occurs until Day 56, when the MC-S-304 specimen reports a minimum i_{corr} of 0.0028 μA/cm^2, from this point, the values stabilize in the range between 0.0039 and 0.0047 μA/cm^2 between Days 112 and 196 of exposure the aggressive medium. Subsequently, the i_{corr} increases gradually from 0.0054 μA/cm^2 on Day 224 to the highest value in the entire exposure period at the end of monitoring, Day 364, with an i_{corr} value of 0.0106 μA/cm^2. As indicated previously, its performance was excellent in the presence of sodium sulfates, with i_{corr} values well below 0.1 μA/cm^2, which is the limit that would indicate the onset of corrosion according to Table 8. This resistance to corrosion of AISI 304 steel embedded in concrete exposed to aggressive media has been demonstrated in various studies [98–100].
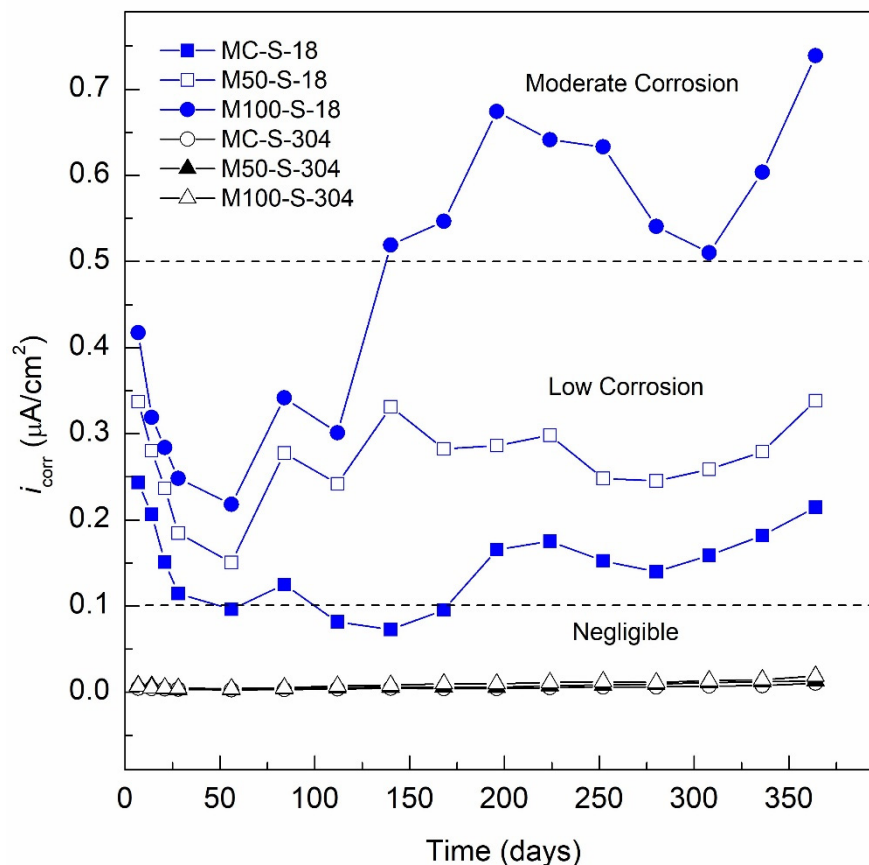
Figure 7. i_{corr} specimens exposed 3.5 wt.% Na_2SO_4 solution (aggressive medium).

In the case of the M50-S-304 specimen, it has a much higher anticorrosive efficiency than that presented by the specimen reinforced with AISI 1018 CS steel (M50-S-18). The M50-S-304 specimen presents i_{corr} values in the curing stage ranging from 0.0080 and 0.0031 μA/cm² from Days 7 to 28, respectively. Day 56 shows an i_{corr} value of 0.0032 μA/cm², an increase in i_{corr} from Day 56 to 196, with constant increases from Days 56 to 112 going from an i_{corr} value of 0.0032 and 0.0052 μA/cm², from there to stabilize and oscillate in the range of 0.0058 and 0.0061 μA/cm². From Day 140 to 196, there is a constant increase until the end of the monitoring period, from an i_{corr} value of 0.0077 μA/cm² on Day 224 to 0.1321 μA/cm² for the Day 364. Like the MC-S-304 specimen, the i_{corr} values are much lower than 0.1 μA/cm², which indicates that its corrosion level is negligible, or passivity occurs, according to the provisions of Table 8. However, it can be observed that the M50-S-304 specimen presents higher values than those reported by the MC-S-304 specimen. This behavior is associated with a less dense and more permeable concrete matrix due to the presence of RCA, as reported by Cakir et al. The compressive strength of the concrete decreases by incorporating RCA and that the presence of RCA causes the concrete to have a higher porosity and lower density [101]. However, another study concluded that the RCA content in the concrete is found to have a detrimental effect in the compressive strength, but at low replacement concentrations <20%, this effect is negligible [102]. The monitored i_{corr} values for AISI 304 SS during the curing period were 0.0071 and 0.0047 μA/cm² on Days 7 and 28, respectively, during the curing stage. Next, the i_{corr} increases from 0.0041 to 0.0098 μA/cm² for Days 56 to 168, respectively. A second period of increase occurs from Days 196 to 280, from an i_{corr} value of 0.00989 to 0.1143 μA/cm². Finally, the third period with near-constant i_{corr} of 0.01346 μA/cm² on Day 308 to i_{corr} of 0.01894 μA/cm² on Day 364. The i_{corr} values during all the periods of exposure showed values less than 0.1 μA/cm², which indicates an excellent performance against sulfate corrosion for the M100-S-304 specimen with 100% of RCA and 20% of SCBA.

The corrosion resistance was not influenced by the high permeability, low density and low mechanical resistance of the GC with which the M100-S-304 specimen was made. By data fitting, the durability properties generally decrease linearly with the increase of RCA replacement and the average water absorption rate [103]. The concrete containing NA and RCA showed a carbonation rate of 1.8 times higher [104]. The increase in the carbonation depth observed in samples containing RCA could be attributed to the higher permeability of RCA due to the presence of old mortar adhering to the NA and the old interfacial transition zone (ITZ) [105]. The geopolymer RCA, with a higher content of granulated blast furnace slag, had a lower mass loss and a higher residual compressive strength after the sulfate exposure [106]. The results indicate a direct influence between the percentage of aggregate used in the GC mixes and the level of corrosion that all the specimens present in both the control medium and the aggressive medium. Higher contents of RCA lead to higher i_{corr} in both AISI 1018 CS and AISI 304 SS steels. This behavior is the opposite of the reported behavior in another research, where it was found that the influence on the performance against most usual corrosion processes displayed similar results under a natural chloride attack [107]. Therefore, it is of great importance to continue to study different types of reinforcing steels as an alternative to AISI 1018 steel [108,109] that can increase the resistance to corrosion of GC based on recycled aggregates and alternative materials to OPC, such as SCBA, FA and SF.

4. Conclusions

According to the results from the study, the following conclusions were reached:

GC samples showed a significant decrease in the slump in their fresh state, GC-M50 with a slump of 3 cm and GC-M100 with a slump of 2 cm, decreasing their workability compared to conventional concrete (MC) which presented a slump of 10 cm.

The compressive strength shows a decreasing trend as the content of RCA present in GC increases. The GC-M50 mix with 50% RCA and 20% SCBA must be substituted for the CPC 30R. A compressive strength of 11.54 MPa was observed at 28 days, which represents a decrease of 42% with respect to the MC. A decrease of 51.5% for GC with 100% RCA and 20% SCBA replacing CPC 30R. A compressive strength of only 9.66 MPa was seen for Day 28.

The results obtained in the present investigation indicate a direct influence between the percentage of aggregate used in the GC mixes and the level of corrosion that all the specimens present in both the control medium and the aggressive medium, the higher the content of RCA, the higher the corrosion rate in both CS 1018 and AISI 304 SS reinforcements.

The i_{corr} values of the GC specimens reinforced with AISI 304 SS exposed to Na_2SO_4 were found to be 0.01894 $\mu A/cm^2$ on Day 364, two orders of magnitude lower than the i_{corr} values (0.7389 $\mu A/cm^2$) obtained for CS 1018 in the same period. Therefore, it is shown that even with low mechanical properties, less dense concrete matrix and high permeability, the durability of GC is increased by presenting excellent resistance to corrosion when exposed to 3.5 wt.% Na_2SO_4 for more than 364 days, associated with the excellent corrosion performance of AISI 304 SS as reinforcement in concrete exposed to aggressive media.

Conflicts of Interest: The authors declare no conflict of interest.

References

1. Cramer, S.D.; Covino, B.S.; Bullard, S.J.; Holcomb, G.R.; Russell, J.H.; Nelson, F.J.; Laylor, H.M.; Soltesz, S.M. Corrosion prevention and remediation strategies for reinforced concrete coastal bridges. *Cem. Concr. Compos.* **2002**, *24*, 101–117. [CrossRef]

2. Koch, G.H.; Brongers, M.; Neil, G.; Thompson, C.C.; Virmani, P.; Payer, J.H. *Corrosion Costs and Preventive Strategies in the United States*; Publication No. FHWA-RD-01-156; NACE International: Houston, TX, USA, 2002.

3. Güneyisi, E.; Ozturan, T.; Gesoglu, M. A study on reinforcement corrosion and related properties of plain and blended cement concretes under different curing conditions. *Cem. Concr. Compos.* **2005**, *27*, 449–461. [CrossRef]

4. Pin Gu, S.; Beaudoin, J.J.; Arsenault, B. Corrosion resistance of stainless steel in chloride contaminated concrete. *Cem. Concr. Res.* **1996**, *26*, 1151–1156.

5. Saricimen, H.; Mohammad, M.; Quddus, A.; Shameem, M.; Barry, M.S. Effectiveness of concrete inhibitors in retarding rebar corrosion. *Cem. Concr. Compos.* **2002**, *24*, 89–100. [CrossRef]

6. De Rincon, O.T.; Montenegro, J.; Vera, R.; Carvajal, A.; De Gutiérrez, R.M.; Saborio, E.; Acosta, A.A.T.; PãRez-Quiroz, J.; Martinez-Madrid, M.; Martínez-Molina, W.; et al. Reinforced concrete durability in marine environments DURACON Project: Long-term exposure. *Corrosion* **2016**, *72*, 824–833. [CrossRef]

7. Baltazar, M.A.; Márquez, S.; Landa, L.; Croche, R.; López, O. Effect of the type of curing on the corrosion behavior of concrete exposed to urban and marine environment. *Eur. J. Eng. Res. Sci.* **2020**, *5*, 91–95. [CrossRef]

8. Ormellese, M.; Berra, M.; Bolzoni, F.; Pastore, T. Corrosion inhibitors for chlorides induced corrosion in reinforced concrete structures. *Cem. Concr. Res.* **2006**, *36*, 536–547. [CrossRef]

9. Baltazar, M.A.; Santiago, G.; Moreno, V.M.; Croche, R.; De la Garza, M.; Estupiñan, F.; Zambrano, P.; Gaona, G. Electrochemical behaviour of galvanized steel embedded in concrete exposed to sand contaminated with NaCl. *Int. J. Electrochem. Sci.* **2016**, *11*, 10306–10319. [CrossRef]

10. Gowripalan, N.; Mohameda, H.M. Chloride-ion induced corrosion of galvanized and ordinary steel reinforcement in high-performance concrete. *Cem. Concr. Res.* **1998**, *28*, 1119–1131. [CrossRef]

11. Liang, M.; Lan, J.J. Reliability analysis for the existing reinforced concrete pile corrosion of bridge substructure. *Cem. Concr. Res.* **2005**, *35*, 540–550. [CrossRef]

12. Santiago, G.; Baltazar, M.A.; Galindo, A.; Cabral, J.A.; Estupíñan, F.H.; Zambrano, P.; Gaona, C. Anticorrosive Efficiency of Primer Applied in Carbon Steel AISI 1018 as Reinforcement in a Soil Type MH. *Int. J. Electrochem. Sci.* **2013**, *8*, 8490–8501.

13. Elias, V.; Fishman, K.L.; Cristopher, B.R.; Berg, R.R. *Corrosion/Degradation of Soil Reinforcements for Mechanically Stabilized Earth Walls and Reinforced Soil Slopes*; U.S. Department of Transportation Publication No. FHWA-NHI-09-087; Federal Highway Administration: Washington, DC, USA, 2009.

14. Ismail, A.I.M.; El-Shamy, A.M. Engineering behaviour of soil materials on the corrosion of mild steel. *Appl. Clay Sci.* **2009**, *42*, 356–362. [CrossRef]

15. Santiago, G.; Baltazar, M.A.; Galván, R.; López, L.; Zapata, F.; Zambrano, P.; Gaona, C.; Almeraya, F. Electrochemical evaluation of reinforcement concrete exposed to soil type SP contaminated with sulphates. *Int. J. Electrochem. Sci.* **2016**, *11*, 4850–4864. [CrossRef]

16. Baltazar, M.A.; Santiago, G.; Gaona, C.; Maldonado, M.; Barrios, C.P.; Nunez, R.; Perez, T.; Zambrano, P.; Almeraya, F. Evaluation of the corrosion at early age in reinforced concrete exposed to sulfates. *Int. J. Electrochem. Sci.* **2012**, *7*, 588–600.

17. Baltazar-Zamora, M.A.; Landa-Ruiz, L.; Rivera, Y.; Croche, R. Electrochemical evaluation of galvanized steel and AISI 1018 as reinforcement in a soil type MH. *Eur. J. Eng. Res. Sci.* **2020**, *5*, 259–263. [CrossRef]

18. Bellezze, T.; Malavolta, M.; Quaranta, A.; Ruffini, N.; Roventi, G. Corrosion behaviour in concrete of three differently galvanized steel bars. *Cem. Concr. Compos.* **2006**, *28*, 246–255. [CrossRef]

19. Kayali, O.; Yeomans, S. Bond of ribbed galvanized reinforcing steel in concrete. *Cem. Concr. Compos.* **2000**, *22*, 459–467. [CrossRef]

20. Cheng, A.; Huang, R.; Wu, J.K.; Chen, C.H. Effect of rebar coating on corrosion resistance and bond strength of reinforced concrete. *Constr. Build. Mater.* **2005**, *19*, 404–412. [CrossRef]

21. Martin, U.; Ress, J.; Bosch, J.; Bastidas, D.M. Stress corrosion cracking mechanism of AISI 316LN stainless steel rebars in chloride contaminated concrete pore solution using the slow strain rate technique. *Electrochim. Act.* **2020**, *335*, 135565. [CrossRef]

22. Mahasenan, N.; Smith, S.; Humphreys, K. The cement industry and global climate change: Current and potential future cement industry CO_2 emissions. In *Greenhouse Gas Control Technologies, Proceedings of the 6th International Conference, Kyoto, Japan, 1–4 October 2002*; Elsevier: Amsterdam, The Netherlands, 2003; pp. 995–1000.

23. Habert, G.; d'Espinose de Lacaillerie, J.B.; Roussel, N. An environmental evaluation of geopolymer based concrete production: Reviewing current research trends. *J. Clean. Prod.* **2011**, *19*, 1229–1238. [CrossRef]

24. Ariza-Figueroa, H.A.; Bosch, J.; Baltazar-Zamora, M.A.; Croche, R.; Santiago-Hurtado, G.; Landa-Ruiz, L.; Mendoza-Rangel, J.M.; Bastidas, J.M.; Almeraya-Calderón, F.; Bastidas, D.M. Corrosion behavior of AISI 304 stainless steel reinforcements in SCBA-SF ternary ecological concrete exposed to $MgSO_4$. *Materials* **2020**, *13*, 2412. [CrossRef] [PubMed]

25. Franco-Luján, V.A.; Maldonado-García, M.A.; Mendoza-Rangel, J.M.; Montes-García, P. Chloride-induced reinforcing steel corrosion in ternary concretes containing fly ash and untreated sugarcane bagasse ash. *Const. Build. Mater.* **2019**, *198*, 608–618. [CrossRef]

26. Kupwade-Patil, K.; Allouche, E.N. Examination of chloride-induced corrosion in reinforced geopolymer concretes. *J. Mater. Civil Eng.* **2013**, *25*, 1465–1476. [CrossRef]

27. Gunasekara, C.; Law, D.W.; Setunge, S. Long term permeation properties of different fly ash geopolymer concretes. *Const. Build. Mater.* **2016**, *124*, 352–362. [CrossRef]

28. Ganesan, K.; Rajagopal, K.; Thangavel, K. Evaluation of bagasse ash as corrosion resisting admixture for carbon steel in concrete. *Anti-Corros. Methods Mater.* **2007**, *54*, 230–236. [CrossRef]

29. Amin, N.U. Use of bagasse ash in concrete and its impact on the strength and chloride resistivity. *J. Mater. Civil Eng.* **2011**, *23*, 717–720. [CrossRef]

30. Somna, R.; Jaturapitakkul, C.; Rattanachu, P.; Chalee, W. Effect of ground bagasse ash on mechanical and durability properties of recycled aggregate concrete. *Mater. Des.* **2012**, *36*, 597–603. [CrossRef]

31. Cordeiro, G.C.; Toledo Filho, R.D.; Tavares, L.M.; Fairbairn, E.M.R. Experimental characterization of binary and ternary blended-cement concretes containing ultrafine residual rice husk and sugar cane bagasse ashes. *Constr. Build. Mater.* **2012**, *29*, 641–646. [CrossRef]

32. Rukzon, S.; Chindaprasirt, P. Utilization of bagasse ash in high-strength concrete. *Mater. Des.* **2012**, *34*, 45–50. [CrossRef]

33. Baltazar-Zamora, M.A.; Ariza-Figueroa, H.; Landa-Ruiz, L.; Croche, R. Electrochemical evaluation of AISI 304 SS and galvanized steel in ternary ecological concrete based on sugar cane bagasse ash and silica fume (SCBA-SF) exposed to Na_2SO_4. *Eur. J. Eng. Res. Sci.* **2020**, *5*, 353–357. [CrossRef]

34. Padhi, R.; Mukharjee, B. Effect of rice husk ash on compressive strength of recycled aggregate concrete. *J. Basic Appl. Eng. Res* **2017**, *4*, 356–359.

35. Joshaghani, A.; Moeini, M.A. Evaluating the effects of sugar cane bagasse ash (SCBA) and nanosilica on the mechanical and durability properties of mortar. *Constr. Build. Mater.* **2017**, *152*, 818–831.

36. Jagadesh, P.; Ramachandramurthy, A.; Murugesan, R.; Karthik Prabhu, T. Adaptability of sugar cane bagasse ash in mortar. *J. Inst. Eng. India Ser. A* **2019**, *100*, 225–240.

37. Praveenkumar, S.; Sankarasubramanian, G. Mechanical and durability properties of bagasse ash-blended high-performance concrete. *SN Appl. Sci.* **2019**, *1*, 1664.

38. Ojeda, O.; Mendoza, J.M.; Baltazar, M.A. Influence of sugar cane bagasse ash inclusion on compacting, CBR and unconfined compressive strength of a subgrade granular material. *Rev. Alconpat* **2018**, *8*, 194–208.

39. Ganesan, K.; Rajagopal, K.; Thangavel, K. Evaluation of bagasse ash as supplementary cementitious material. *Cem. Concr. Compos.* **2007**, *29*, 515–524.

40. Chusilp, N.; Jaturapitakkul, C.; Kiattikomol, K. Effects of LOI of ground bagasse ash on the compressive strength and sulfate resistance of mortars. *Constr. Build. Mater.* **2009**, *23*, 3523–3531.

41. Turner, L.K.; Collins, F.G. Carbon dioxide equivalent (CO_2-e) emissions: A comparison between geopolymer and OPC cement concrete. *Constr. Build. Mater.* **2013**, *43*, 125–130.

42. Talha Junaid, M.; Kayali, O.; Khennane, A.; Black, J. A mix design procedure for low calcium alkali activated fly ash-based concretes. *Constr. Build. Mater.* **2015**, *79*, 301–310.

43. Pawluczuk, E.; Kalinowska-Wichrowska, K.; Boltryk, M.; Ramón, J.; Fernandez, J. The influence of heat and mechanical treatment of concrete rubble on the properties of recycled aggregate concrete. *Materials* **2019**, *12*, 367.

44. Fraile García, E.; Ferreiro-Cabello, J.; López-Ochoa, L.M.; López Gonzáles, L.M. Study of the technical feasibility of increasing the amount of recycled concrete waste used in ready-mix concrete production. *Materials* **2017**, *10*, 817. [CrossRef]

45. Dhir, R.; Henderson, N.; Limbachiya, M. *Proceedings of International Symposium: Sustainable Construction: Use of Recycled Concrete Aggregate*; Thomas Telford Ltd.: London, UK, 2015.

46. De Vries, P. Concrete recycled: Crushed concrete aggregate. In *Concrete in the Service of Mankind. I. Concrete for Environment Enhancement and Protection, Proceedings of the International Conference, Dundee, UK, 24–26 June 1996*; E & FN Spon: London, UK; New York, NY, USA, 1996; pp. 121–130.

47. Limbachiya, M.C.; Leelawat, T.; Dhir, R.K. Use of recycled concrete aggregate in high-strength concrete. *Mater. Struct.* **2000**, *33*, 574–580.

48. Oikonomou, N.D. Recycled concrete aggregates. *Cem. Concr. Compos.* **2005**, *27*, 315–318.

49. Berndt, M.L. Properties of sustainable concrete containing fly ash, slag and recycled concrete aggregate. *Constr. Build. Mater* **2009**, *23*, 2606–2613.

50. Landa-Gómez, A.E.; Croche, R.; Márquez-Montero, S.; Villegas Apaez, R.; Ariza-Figueroa, H.A.; Estupiñan López, F.; Gaona Tiburcio, G.; Almeraya Calderón, F.; Baltazar-Zamora, M.A. Corrosion behavior 304 and 316 stainless steel as reinforcement in sustainable concrete based on sugar cane bagasse ash exposed to Na_2SO_4. *ECS Trans.* **2018**, *84*, 179–188. [CrossRef]

51. Chusilp, N.; Jaturapitakkul, C.; Kiattikomol, K. Utilization of bagasse ash as a pozzolanic material in concrete. *Constr. Build. Mater.* **2009**, *23*, 3352–3358. [CrossRef]

52. Khan, K.; Ullah, M.F.; Shahzada, K.; Amin, M.; Bibi, T.; Wahab, N.; Aljaafari, A. Effective use of micro-silica extracted from rice husk ash for the production of high-performance and sustainable cement mortar. *Constr. Build. Mater.* **2020**, *258*, 119589.

53. Akram, T.; Memon, S.; Obaid, H. Production of low cost self compacting concrete using bagasse ash. *Constr. Build. Mater.* **2009**, *23*, 703–712.

54. Yashwanth, M.K.; Naresh, B.G.; Sandeep, D.S. Potential of bagasse ash as alternative cementitious material in recycled aggregate concrete. *Int. J. Innov. Technol. Explor. Eng.* **2019**, *8*, 271–275.

55. Zhao, Y.; Dong, J.; Wu, Y.; Wang, H.; Li, X.; Xu, Q. Steel corrosion and corrosion-induced cracking in recycled aggregate concrete. *Corros. Sci.* **2014**, *85*, 241–250.

56. Liang, C.; Ma, H.; Pan, Y.; Ma, Z.; Duan, Z.; He, Z. Chloride permeability and the caused steel corrosion in the concrete with carbonated recycled aggregate. *Constr. Build. Mater.* **2019**, *218*, 506–518. [CrossRef]

57. Qing, X.; Tao, J.; San-Ji, G.; Zhengxian, Y.; Nengsen, W. Characteristics and Applications of Sugar Cane Bagasse Ash Waste in Cementitious Materials. *Materials* **2019**, *12*, 1–19.

58. *ACI 211.1-91 Standard. Standard Practice for Selecting Proportions for Normal, Heavyweight, and Mass Concrete*; ACI: Farmington Hills, MI, USA, 2002.

59. *NMX-C-414-ONNCCE-2014–Industria de la Construcción—Cementantes Hidráulicos–Especificaciones y Métodos de Ensayo*; ONNCCE, Cd.: Mexico City, Mexico, 2014.

60. *ASTM C127–15–Standard Test Method for Relative Density (Specific Gravity) and Absorption of Coarse Aggregate*; ASTM International: West Conshohocken, PA, USA, 2015.

61. *ASTM C128–15–Standard Test Method for Relative Density (Specific Gravity) and Absorption of Fine Aggregate*; ASTM International: West Conshohocken, PA, USA, 2015.

62. *ASTM C29/C29M–07–Standard Test Method for Bulk Density ("Unit Weight") and Voids in Aggregate*; ASTM International: West Conshohocken, PA, USA, 2007.

63. *ASTM C33/C33M–16e1–Standard Specification for Concrete Aggregates*; ASTM International: West Conshohocken, PA, USA, 2016.

64. *ACI 214R-11 Standard, Guide to Evaluation of Strength Test Results of Concrete*; ACI: Farmington Hills, MI, USA, 2011.

65. *NMX-C-156-ONNCCE-2010–Determinacion de Revenimiento en Concreto Fresco*; ONNCCE, Cd.: Mexico City, Mexico, 2010.

66. *ASTM C 1064/C1064M–08–Standard Test Method for Temperature of Freshly Mixed Hydraulic-Cement Concrete*; ASTM International: West Conshohocken, PA, USA, 2008.

67. *NMX-C-162-ONNCCE-2014–Industria de la Construcción—Concreto Hidráulico—Determinación de la Masa Unitaria, Cálculo del Rendimiento y Contenido de Aire del Concreto Fresco por el Método Gravimétrico*; ONNCCE, Cd.: Mexico City, Mexico, 2014.

68. *NMX-C-083-ONNCCE-2014–Industria de la Construcción—Concreto–Determinación de la Resistencia a la Compresión de Especímenes—Método de Ensayo*; ONNCCE, Cd.: Mexico City, Mexico, 2014.

69. Ali, B.; Qureshi, L.; Raza, A.; Nawaz, M.; Rehman, S.; Rashid, M. Influence of glass fibers on mechanical properties on concrete with recycled coarse aggregate. *Civil Eng. J.* **2019**, *5*, 1007–1019. [CrossRef]

70. Kurda, R.; De Brito, J.; Silvestre, J. Combined economic and mechanical performance optimization of recycled aggregate concrete with high volume of fly ash. *Appl. Sci.* **2018**, *8*, 1189. [CrossRef]

71. Castaldelli, N.; Moraes, J.C.B.; Akasaki, J.L.; Melges, J.L.P.; Monzó, J.; Borrachero, M.V.; Soriano, L.; Payá, J.; Tashima, M.M. Study of the binary system fly ash/sugarcane bagasse ash (FA/SCBA) in SiO$_2$/K$_2$O alkali-activated binders. *Fuel* **2016**, *174*, 307–316. [CrossRef]

72. Li, W.; Xiao, J.; Shi, C.; Poon, C. Structural behaviour of composites members with recycled aggregate concrete—An overview. *Adv. Struct. Eng.* **2015**, *18*, 919–938. [CrossRef]

73. Landa, A.E.; Croche, R.; Márquez, S.; Galván, R.; Gaona, C.; Almeraya, F.; Baltazar, M.A. Correlation of compression resistance and rupture module of a concrete of ratio w/c = 0.50 with the corrosion potential, electrical resistivity and ultrasonic pulse speed. *ECS Trans.* **2018**, *84*, 217–227. [CrossRef]

74. Volpi-León, V.; López-Léon, L.D.; Hernández-Ávila, J.; Baltazar-Zamora, M.A.; Olguín-Coca, F.J.; López-León, A.L. Corrosion study in reinforced concrete made with mine waste as mineral additive. *Int. J. Electrochem. Sci.* **2017**, *12*, 22–31. [CrossRef]

75. Santiago, G.; Baltazar, M.A.; Olguín, J.; López, L.; Galván, R.; Ríos, A.; Gaona, C.; Almeraya, F. Electrochemical evaluation of a stainless steel as reinforcement in sustainable concrete exposed to chlorides. *Int. J. Electrochem. Sci.* **2016**, *11*, 2994–3006. [CrossRef]

76. *ASTM C192/C192M–16a–Standard Practice for Making and Curing Concrete Test Specimens in the Laboratory*; ASTM International: West Conshohocken, PA, USA, 2016.

77. *NMX-C-159-ONNCCE-2004, Industria de la Construcción—Concreto—Elaboración y Curado de Especímenes en ONNCCE S.C., Cd.*; ONNCCE, Cd.: Mexico City, Mexico, 2004.

78. Liang, M.; Lin, L.; Liang, C. Service Life Prediction of Existing Reinforced Concrete Bridges Exposed to Chloride Environment. *J. Infrastruct. Syst.* **2002**, *8*, 76–85. [CrossRef]

79. Pradhan, B. Corrosion behavior of steel reinforcement in concrete exposed to composite chloride–sulfate environment. *Constr. Build. Mater.* **2014**, *72*, 398–410.

80. *ASTM G 59-97 (2014)–Standard Test Method for Conducting Potentiodynamic Polarization Resistance Measurements*; ASTM International: West Conshohocken, PA, USA, 2014.

81. Fajardo, S.; Bastidas, D.M.; Criado, M.; Romero, M.; Bastidas, J.M. Corrosion behaviour of a new low-nickel stainless steel in saturated calcium hydroxide solution. *Constr. Build. Mater.* **2011**, *25*, 4190–4196.

82. Baltazar, M.A.; Maldonado, M.; Tello, M.; Santiago, G.; Coca, F.; Cedano, A.; Barrios, C.P.; Nuñez, R.; Zambrano, P.; Gaona, C.; et al. Efficiency of galvanized steel embedded in concrete previously contaminated with 2, 3 and 4% of NaCl. *Int. J. Electrochem. Sci.* **2012**, *7*, 2997–3007.

83. Andrade, C.; Alonso, C. Corrosion rate monitoring in the laboratory and on-site. *Constr. Build Mater.* **1996**, *10*, 315–328.

84. Feliu, S.; González, J.A.; Andrade, C. Electrochemical Methods for On-Site Determinations of Corrosion Rates of Rebars. In *Techniques to Assess the Corrosion Activity of Steel Reinforced Concrete Structures*; ASTM STP 1276; Berke, N.S., Escalante, E., Nmai, C.K., Whiting, D., Eds.; ASTM International: West Conshohocken, PA, USA, 1996; pp. 107–118.

85. González, J.A.; Ramírez, E.; Bautista, A.; Feliú, S. The behaviour of pre-rusted steel in concrete. *Cem. Concr. Res.* **1996**, *26*, 501–511. [CrossRef]

86. *ASTM C 876-15 (2015)–Standard Test Method for Corrosion Potentials of Uncoated Reinforcing Steel in Concrete*; ASTM International: West Conshohocken, PA, USA, 2015.

87. Al-Yaqout, A.; El-Hawary, M.; Nouh, K.; Khan, P. Corrosion resistance of recycled aggregate concrete incorporating slag. *ACI-Mater. J.* **2020**, *117*, 111–122.

88. Baltazar, M.A.; Landa, A.; Landa, L.; Ariza, H.; Gallego, P.; Ramírez, A.; Croche, R.; Márquez, S. Corrosion of AISI 316 stainless steel embedded in sustainable concrete made with sugar cane bagasse ash (SCBA) exposed to marine environment. *Eur. J. Eng. Res. Sci.* **2020**, *5*, 127–131.

89. García-Alonso, M.C.; González, J.A.; Miranda, J.; Escudero, M.L.; Correia, M.J.; Salta, M.; Bennani, A. Corrosion behaviour of innovative stainless steels in mortar. *Cem. Concr. Res.* **2007**, *37*, 1562–1569. [CrossRef]

90. Lovato, P.; Possan, E.; Coitinho, D.; Masuero, A. Modeling of mechanical properties and durability of recycled aggregate concretes. *Constr. Build. Mater.* **2012**, *26*, 437–447.

91. Bautista, A.; Blanco, G.; Velasco, F. Corrosion behaviour of low-nickel austenitic stainless steels reinforcements: A comparative study in simulated pore solutions. *Cem. Concr. Res.* **2006**, *36*, 1922–1930.

92. Alonso, M.C.; Luna, F.J.; Criado, M. Corrosion behavior of duplex stainless steel reinforcement in ternary binder concrete exposed to natural chloride penetration. *Constr. Build. Mater.* **2019**, 385–395. [CrossRef]

93. Kurda, R.; De Brito, J.; Silvestre, J. Water absorption and electrical resistivity of concrete with recycled concrete aggregates and fly ash. *Cem. Concr. Compos.* **2019**, *95*, 169–182. [CrossRef]

94. Hren, M.; Kosec, T.; Legat, A. Characterization of stainless steel corrosion processes in mortar using various monitoring techniques. *Constr. Build. Mater.* **2019**, *221*, 604–613. [CrossRef]

95. Serdar, M.; Valek, L.; Bjegovic, D. Long-term corrosion behaviour of stainless reinforcing steel in mortar exposed to chloride environment. *Corros. Sci.* **2013**, *69*, 149–157. [CrossRef]

96. Kou, S.; Poon, C.; Agrela, F. Comparasions of natural and recycled aggregate concretes prepared with addition of different mineral admixtures. *Cem. Concr. Compos.* **2011**, *33*, 788–795. [CrossRef]

97. Alhawat, M.; Ashour, A. Bond strength between corroded steel reinforcement and recycled aggregate concrete. *Structures* **2019**, *19*, 369–385. [CrossRef]

98. Bautista, A.; Velasco, F.; Torres-Carrasco, M. Influence of the alkaline reserve of chloride-contaminated mortars on the 6-year corrosion behavior of corrugated UNS S32304 and S32001 stainless steels. *Metals* **2019**, *9*, 686. [CrossRef]

99. Baltazar, M.A.; Bastidas, D.M.; Santiago, G.; Mendoza, J.M.; Gaona, C.; Bastidas, J.M.; Almeraya, F. Effect of silica fume and fly ash admixtures on the corrosion behavior of AISI 304 embedded in concrete exposed in 3.5% NaCl solution. *Materials* **2019**, *12*, 4007. [CrossRef]

100. Criado, M.; Bastidas, D.M.; Fajardo, S.; Fernández-Jiménez, A.; Bastidas, J.M. Corrosion behaviour of a new low-nickel stainless steel embedded in activated fly ash mortars. *Cem. Concr. Compos.* **2011**, *33*, 644–652. [CrossRef]

101. Cakir, O. Experimental analysis of properties of recycled coarse aggregate (RCA) concrete with mineral additives. *Constr. Build. Mater.* **2014**, *68*, 17–25. [CrossRef]

102. Li, X. Recycling and reuse of waste concrete in China: Part I. Material behaviour of recycled aggregate concrete. *Resour. Conserv. Recycl.* **2008**, *53*, 36–44. [CrossRef]

103. Ma, Z.; Tang, Q.; Yang, D.; Ba, G. Durability studies on the recycled aggregate concrete in China over the past decade: A review. *Adv. Civil Eng.* **2019**, *2019*, 4073130. [CrossRef]

104. Pacheco, F.; Miraldo, S.; Labrincha, J.; De Brito, J. An overview on conrete carbonation in the context of eco-efficient construction: Evaluation, Use of SCMs and/or RAC. *Constr. Build. Mater.* **2012**, *36*, 141–150. [CrossRef]

105. Roa, A.; Jha, K.; Misra, S. Use of aggregates from recycled construction and demolition waste in concrete. *Resour. Conserv. Recycl.* **2007**, *50*, 71–81.

106. Xie, J.; Zhao, J.; Wang, J.; Wasn, C.; Huang, P.; Fang, C. Sulfate resistance of recycled aggregate concrete with GGBS and fly ash-based geopolymer. *Materials* **2019**, *12*, 1247. [CrossRef] [PubMed]

107. Gurdian, H.; García, E.; Baeza, F.; Garcés, P.; Zornoza, E. Corrosion behavior of steel reinforcement in concrete with recycled aggregate, fly ash and spent cracking catalyst. *Materials* **2014**, *7*, 3176–3197. [CrossRef]

108. Baltazar, M.A.; Mendoza, J.M.; Croche, R.; Gaona, C.; Hernández, C.; López, L.; Olguín, F.; Almeraya, F. Corrosion behavior of galvanized steel embedded in concrete exposed to soil type MH contaminated with chlorides. *Front. Mater.* **2019**, *6*, 257. [CrossRef]

109. Saravanan, K.; Sathiyanarayanan, S.; Muralidharan, S.; Syed-Azim, S.; Venkatachari, G. Performance evaluation of polyaniline pigmented epoxy coating for corrosion protection of steel in concrete environment. *Prog. Org. Coat.* **2007**, *59*, 160–167. [CrossRef]